Performance Comparison Between SiC and Si Inverter Modules in an Electrical Variable Transmission Application

Mauricio Dalla Vecchia*, Simon Ravyts*, Florian Verbelen+, Jeroen Tant*,
Peter Sergeant+ and Johan Driesen*
*KU Leuven - EnergyVille - Dept. Electrical Engineering (ESAT), Div. ELECTA
*Kasteelpark Arenberg 10, bus 2445
*Leuven, Belgium
+Department of Electromechanical, Systems and Metal Engineering
+FlandersMake@UGent, Belgium
Email: simon.ravyts@kuleuven.be
URL: https://www.energyville.be

Keywords

≪SiC MOSFET≫, ≪DC/AC inverter≫, ≪EVT≫, ≪HEV≫

Abstract

This paper evaluates the performance of Silicon Carbide MOSFET and Silicon IGBT modules in a three-phase inverter for Electrical Variable Transmission systems. For this purpose, two practical inverter set-ups were developed and compared. An increase of several percentage points is visible over the entire operating range for the Silicon Carbide prototype. The total energy efficiency increased by 3.7% for the rotor and by 11.2% for the stator, for the same test conditions.

Introduction

Governments all over the world are forcing the automotive industry, via legislation, to enhance their drive trains in order to reduce fuel consumption and emissions. One of the solutions to increase the efficiency of the traditional Internal Combustion Engine (ICE) based vehicle is to enhance the drive train with a power split transmission. A well know example of such a vehicle, also known as a Hybrid Electrical Vehicle (HEV) is the Toyota Prius. Due to this power split, the ICE can be operated independently from the requested power at the wheels. As a consequence, the operating points of the ICE can be chosen at the optimal operating line. Important side-effects are friction and thus wear in the planetary gears that enable this power split. Moreover, valuable space is taken by the electrical machines that support the traction of the vehicle.

To eliminate the planetary gear, a component can be used that is called the Electrical Variable Transmission (EVT) [1, 2]. The device consists of an inner rotor, an outer rotor and a stator of which the inner rotor and stator are equipped with a distributed three-phase winding [3]. In a HEV, the ICE is connected to the inner rotor while the wheels are connected to the outer rotor [4]. Both shafts are electrically coupled via inverters and the DC-bus, which includes a storage device (i.e. battery). Power can thus be transferred from inner rotor to outer rotor by means of an electric and/or electromagnetic path. Because the power is converted via two separate paths, the EVT can be considered as a power split device.

Wide Band-Gap (WBG) semiconductors are on the rise nowadays and impacts the transportation industry [5]. Gallium Nitride (GaN) and Silicon Carbide (SiC) stand out among the other WBG materials for applications in power electronics. For low voltage/low power applications, GaN proves to be a competitor to the state-of-the-art Si MOSFET technology in applications of, for instance, photovoltaics, battery

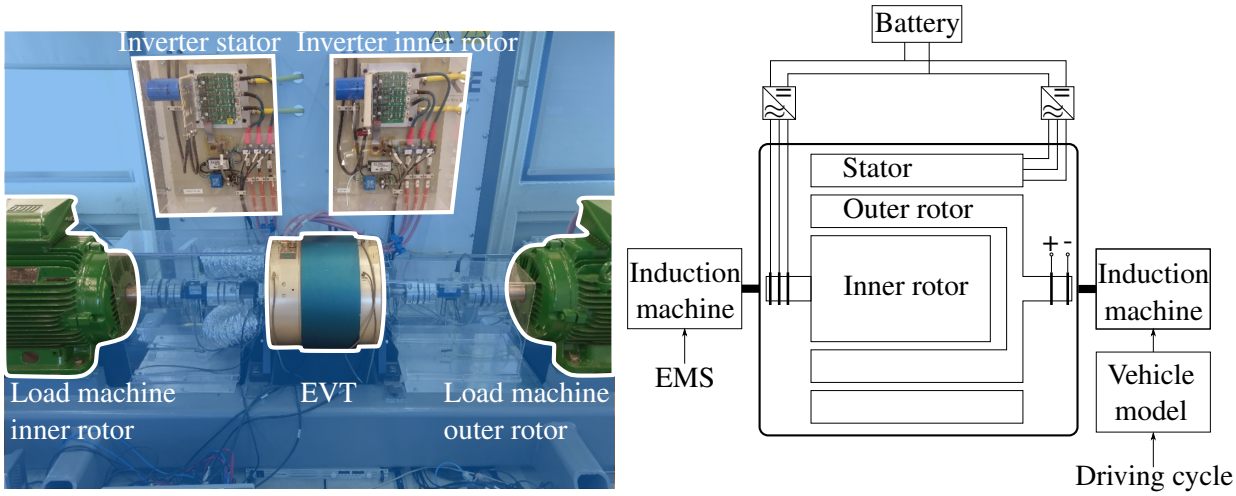

Fig. 1: Experimental setup (left hand side) as well as a schematic representation (right hand side).

energy storage systems or fuel cells [6]. SiC, on the other hand, is considered as a competitor for Si IGBTs for high voltage/ high power applications [7]. The drawbacks of SiC is mainly found in higher component costs, increased ElectroMagnetic Interference (EMI) due to the high di/dt and dv/dt that occur at the switching instants and the lower short-circuit tolerance, requiring faster gate drivers [8].

In general, WBG semiconductors present better electrical characteristics compared to state-of-the-art Si technology. Therefore, the aim of this paper is to develop and experimentally validate the performance, in terms of efficiency, of two DC-AC inverters for use in EVT. The efficiency of SiC MOSFETs will be compared with state-of-the-art Si IGBT technology. A brief discussion about the system under study is presented first, followed by a description of the inverter and experimental results that highlight the superior performance of WBG semiconductors.

System description

The EVT is an electrical machine that consists of an inner rotor, an outer rotor and a stator (see right hand side Fig. 1). Both the inner rotor as the stator are equipped with a distributed three-phase winding. The outer rotor has a single layer of permanent magnet material and a flux bridge, located underneath the DC-field winding (see Fig. 2).

Due to the flux bridge only a part of the permanent magnet flux is linked with the stator. Consequently, the stator flux linkage is low as well as the stator torque. The stator is thus inherently flux weakened as the magnetic field of the magnets links almost completely with the inner rotor. The advantage of this layout is that the induced losses in the stator by the PM field are low as well [9].

During the occasion that high stator torque is required, i.e. high acceleration or higher loads due to uphill driving, the DC-field current can be adapted to increase the stator flux linkage. Note that while the stator flux linkage can be modulated, the inner rotor flux linkage remains invariant for variations of the DC-field current [9].

As the DC-field winding has an impact on both the losses as the actual maximum stator torque, defining the optimal current setpoint is crucial for the performance of the EVT based HEV. To find this optimal current setpoint and in addition the current setpoints in stator and inner rotor for given inner rotor and stator torque, an algorithm is developed to track the optimum (in terms of losses) offline [10]. The results are stored in a look-up table and are used at the setup as setpoint generator for the currents. To control the currents in the stator and inner rotor, two three-phase inverters are used with a common DC-bus (see Fig. 1, left hand side). More details on the inverters are given in the next section. The current in the DC-field winding is controlled via a DC source.

In order to load the shafts of the EVT, two induction machines are used (see Fig. 1, left hand side). These

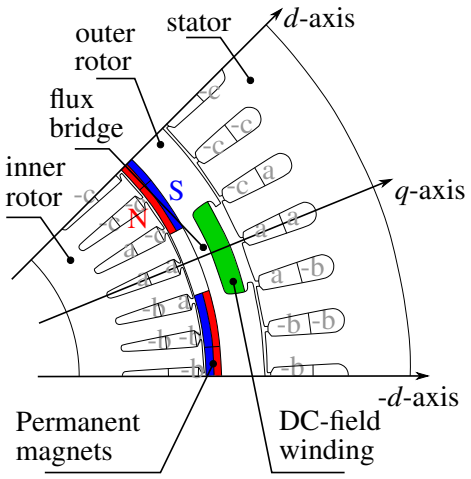

Fig. 2: Cross-sectional view of the EVT considered [11].

Table I: Electrical properties of the tested power modules.

	Si SKiM459GD12E4	SiC CAS300M12BM2
V_{DS}	1200 V	1200 V
$V_{CE,sat}$	1.85 V	/
R_{CE}; $R_{DS,on}$	3.7 mΩ	4.2 mΩ
I_D	452 A @ 70 °C	293 A @ 90 °C
C_{iss}	26.4 nF	19.3 nF
C_{oss}	1.74 nF	2.57 nF
Q_c	2.55 μC	3.2 μC
$t_{d,on}$	276 ns	76 ns
t_r	55 ns	68 ns
$t_{d,off}$	538 ns	168 ns
t_f	114 ns	43 ns

induction machines are controlled with an industrial drive. The induction machine connected to the inner rotor emulates the behavior of an ICE controlled by an Energy Management Strategy (EMS) [12], while the other induction machine emulates the load behavior coming from a vehicle. The set points for both induction machines are generated in a dSPACE platform.

Three-phase inverter

The inverter topology applied in this work is shown in Fig. 3a. A regular three-phase inverter, consisting of three half bridges, is the interface between the battery pack and the inner rotor or stator machine. The battery is emulated by a variable DC power supply. For further comparison between WBG SiC modules and the regular state-of-the-art Si modules, two inverters were tested under the same operational conditions. A space vector modulation scheme for three-phase inverters was implemented and the control signals were generated by a dSPACE module. Both prototypes are also displayed in Figs. 3b and 3c. Fig. 3b shows the Si inverter while Fig. 3c displays the SiC inverter developed for testing purposes and performance comparison. Both prototypes employ water cooling.

The main specification of the Si and SiC modules used in the inverter are shown in Table I. It can be noticed that the WBG SiC module has no forward voltage drop as it is a unipolar device. In contrast, the IGBT is a bipolar switching device with a forward voltage drop $V_{CE,sat}$. Furthermore, the SiC module has improved transient characteristics compared to its Si competitor, which reduces drastically the switching losses under normal operation. The other specifications are comparable and present similar values.

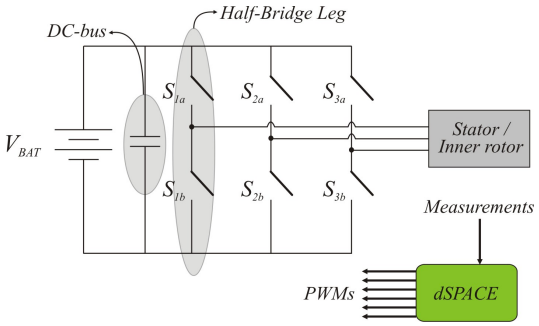

(a) Schematic representation.

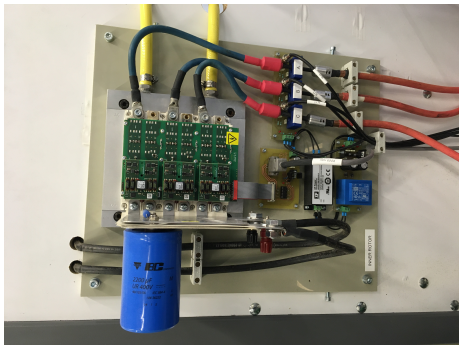

(b) Si IGBT inverter.

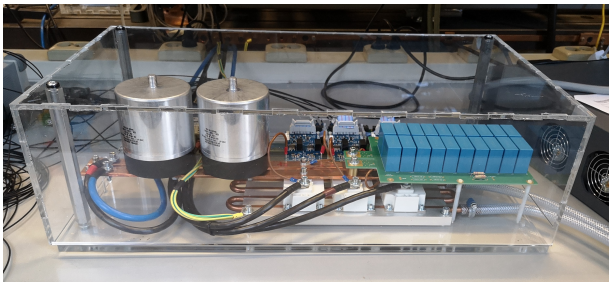

(c) SiC MOSFET inverter.

Fig. 3: Three-phase inverter for interconnection of the battery pack and the inner rotor/stator.

To avoid EMI problems related to the high switching speed of the SiC MOSFETs, the capacitor banks were carefully designed to minimize the stray inductance between the legs and the DC bus. For the bulk capacitance, two 310μF Cornell Dubilier 947D311K132CFRSN film capacitors were used for their low Equivalent Series Resistance (ESR) and inductance (ESL), to guarantee a stable DC-link voltage. Furthermore, an extra film capacitor bank of 75μ F using Epcos M115616276 was placed on top of the SiC power modules to minimize the influence of stray inductances and improve filtering. The implemented driver is the Wolfspeed CGD15HB62P1.

Experimental results

In order to evaluate the performance of the Si and SiC inverters, both are imposed to the same set of power cycles, guaranteeing similar testing conditions. As there are two inverters, one for the stator and one for the rotor, which are typically subjected to different power cycles in a HEV, two power cycles are

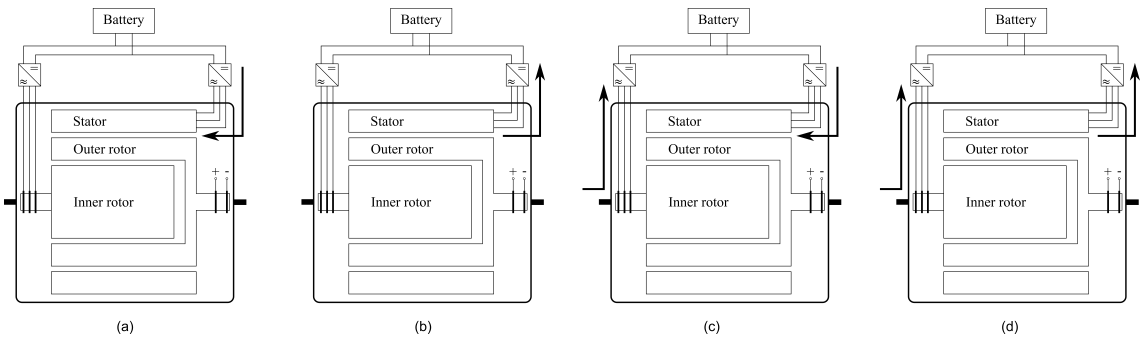

Fig. 4: Considered electrical power flows in the power cycles. The arrows specify the electrical power flow. (a) Mode a: pure electrical driving (acceleration). (b) Mode b: pure electrical driving (regenerative braking). (c) Mode c: charging via ICE while acceleration. (d) Mode (d): charging via ICE as well as due to regenerative braking.

defined. The cycles are characterized by four operational modes that can occur during driving (see Fig. 4). The first 2 modes consider pure electric driving (Fig. 4 (a) and (b), acceleration and regenerative braking, respectively). In the third and fourth mode (Fig. 4 (c) and (d), respectively), the battery is charged via the ICE while the vehicle is being accelerated or decelerated. Please note that the authors are well aware that there are many more possible combinations and that the considered power flows do not necessarily result in the most efficient system level behavior (vehicle). However, enough variability in the power flow is considered to benchmark the SiC inverter with the Si inverter.

The operational switching frequency was defined as f_s = 10 kHz and a peak power of 10 kW is processed. In Figs. 5, 6, 7 and 8, the measured currents, the processed power, the losses and the instantaneous efficiency are plotted over the time duration of the implemented torque profile. The measurements were done using a Yokogawa WT1800 power analyzer. For a driving cycle of about 20 minutes, one measure per 50ms is acquired which leads to a total of about 24 thousand points measured per test (all points displayed in the measured Figures). Not only the measured datapoints but also the calculated error bars are displayed. The error was calculated using standard methods for uncertainty analysis [13] and consider the scale/range of the measurements.

The experimental results are shown four times: twice for the Si and SiC test of the rotor and twice for the Si and SiC test of the stator. A measured negative electrical power in the inverter connected to the inner rotor windings means that power is flowing from the emulated ICE to the battery (mode c and d displayed in Fig. 4). For the stator, a positive power flow means acceleration of the vehicle (mode a or c displayed in Fig. 4), while a negative power flow means regenerative braking (mode b or d displayed in Fig. 4).

Both for the rotor and stator a significant improvement is visible for the measured losses over the entire torque profile. The reduction in losses leads to a strong efficiency increase, as visible in Fig. 9. The overall energy efficiency was twice improved by implementing SiC MOSFETs and lead to an increase of 3.7% and 11.2% for respectively the rotor and the stator. The results are summarized in Table II. The performance difference between the rotor and stator are a consequence of the defined driving cycle. More reactive power circulate through the inverter connected to the stator.

Table II: Measured energy efficiency (in %) over the pre-defined torque profile.

	Si IGBT	SiC MOSFET	Difference
Rotor	92.9 ± 1.6	96.6 ± 1.7	+3.7
Stator	77.6 ± 2.2	88.8 ± 2.5	+11.2

Conclusions

This works aim at testing the overall performance of Si and SiC inverters operating in an Electrical Variable Transmission system. Under similar testing conditions, the SiC MOSFET inverters present better performance compared with its Si IGBT modules competitor for a 10kHz operational switching frequency and 10kW of processed power. An improvement of around 3.7% and 11.2% is observed for the SiC inverters connected to the inner rotor and stator machines, respectively.

Acknowledgments

This work was carried out for the EMTechno project (project ID: IWT150513) supported by VLAIO and Flanders Make, the strategic research centre for the manufacturing industry in Belgium.

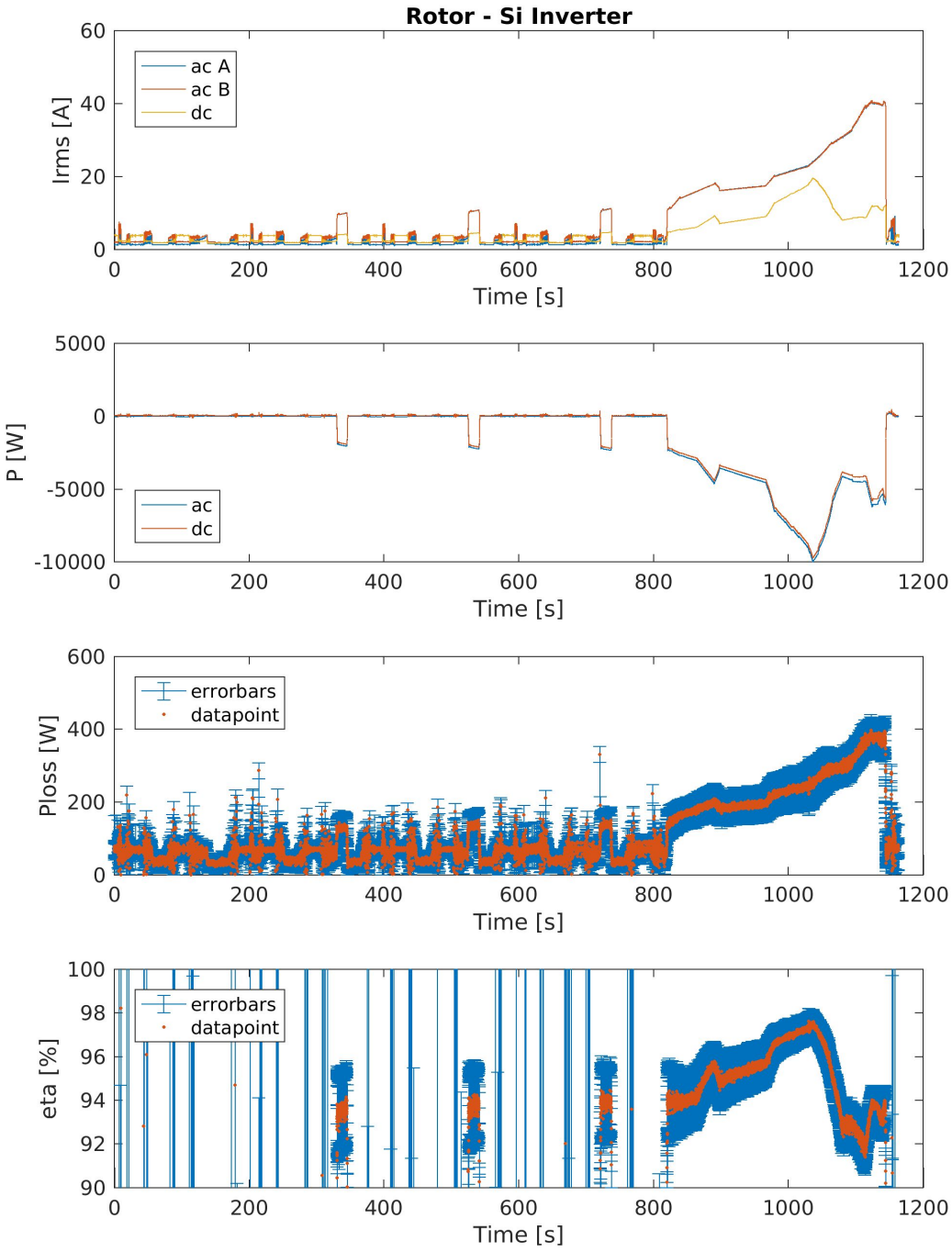

Fig. 5: Performance of the rotor when the Si IGBT inverter is used.

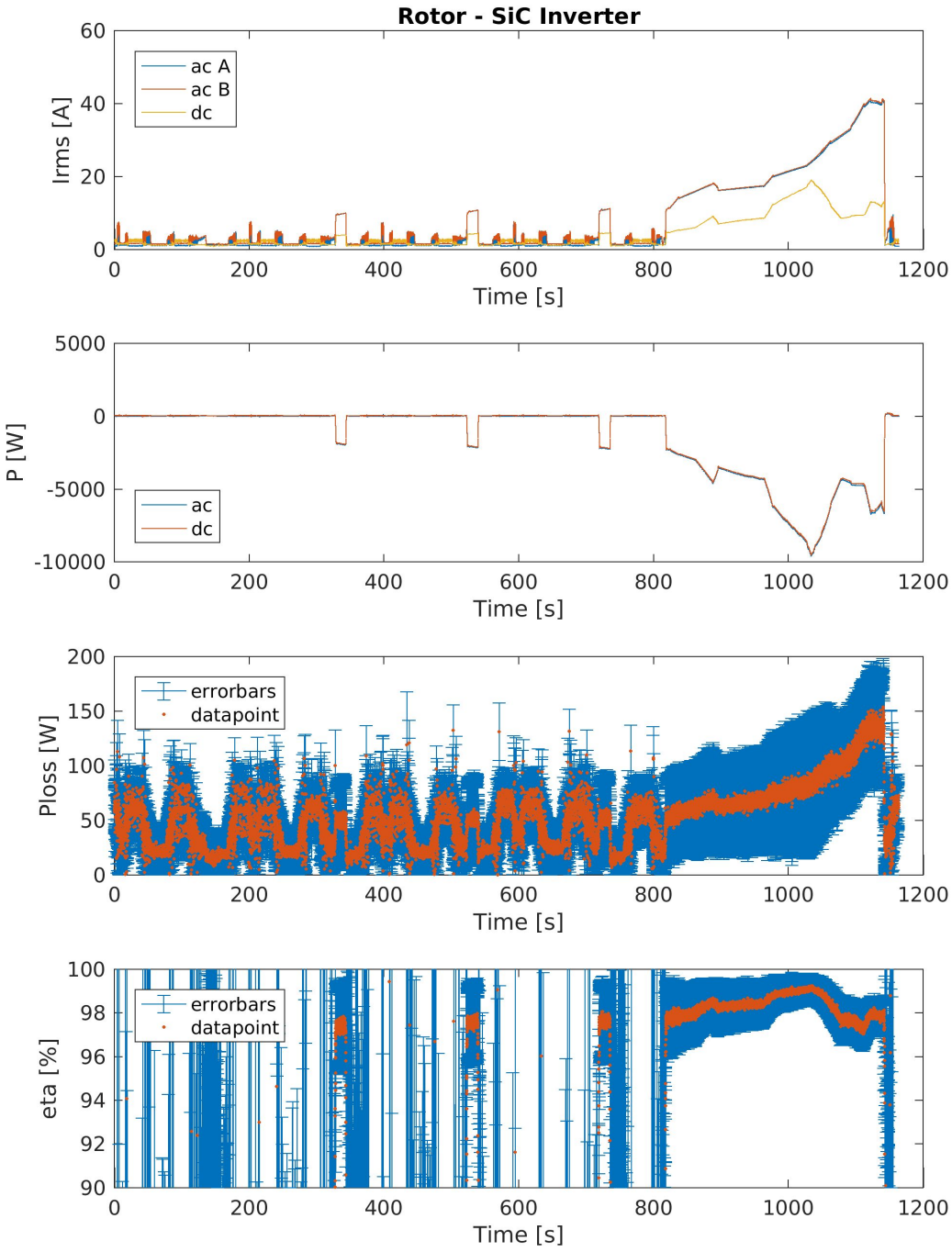

Fig. 6: Performance of the rotor when the SiC MOSFET inverter is used.

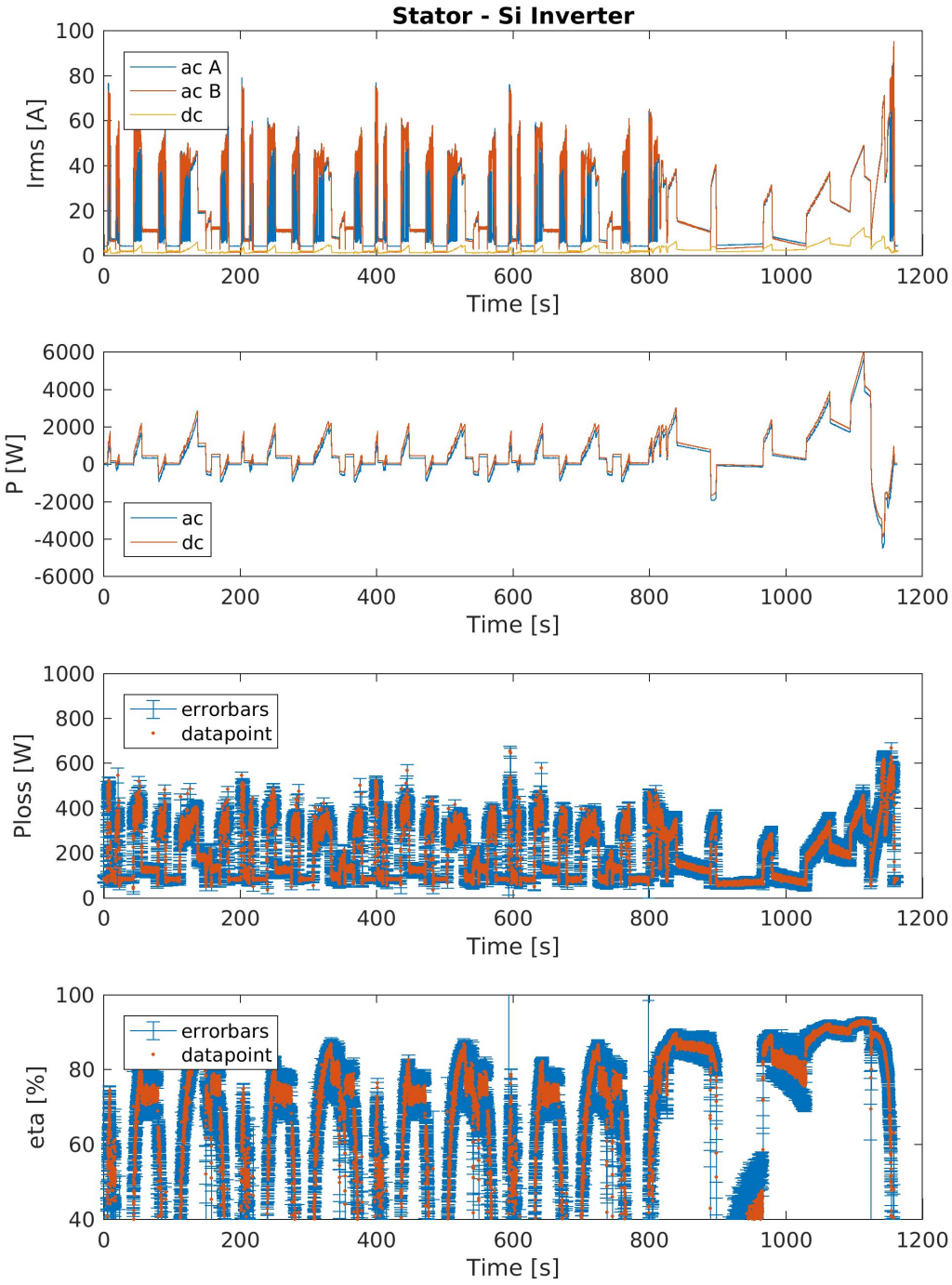

Fig. 7: Performance of the stator when the Si IGBT inverter is used.

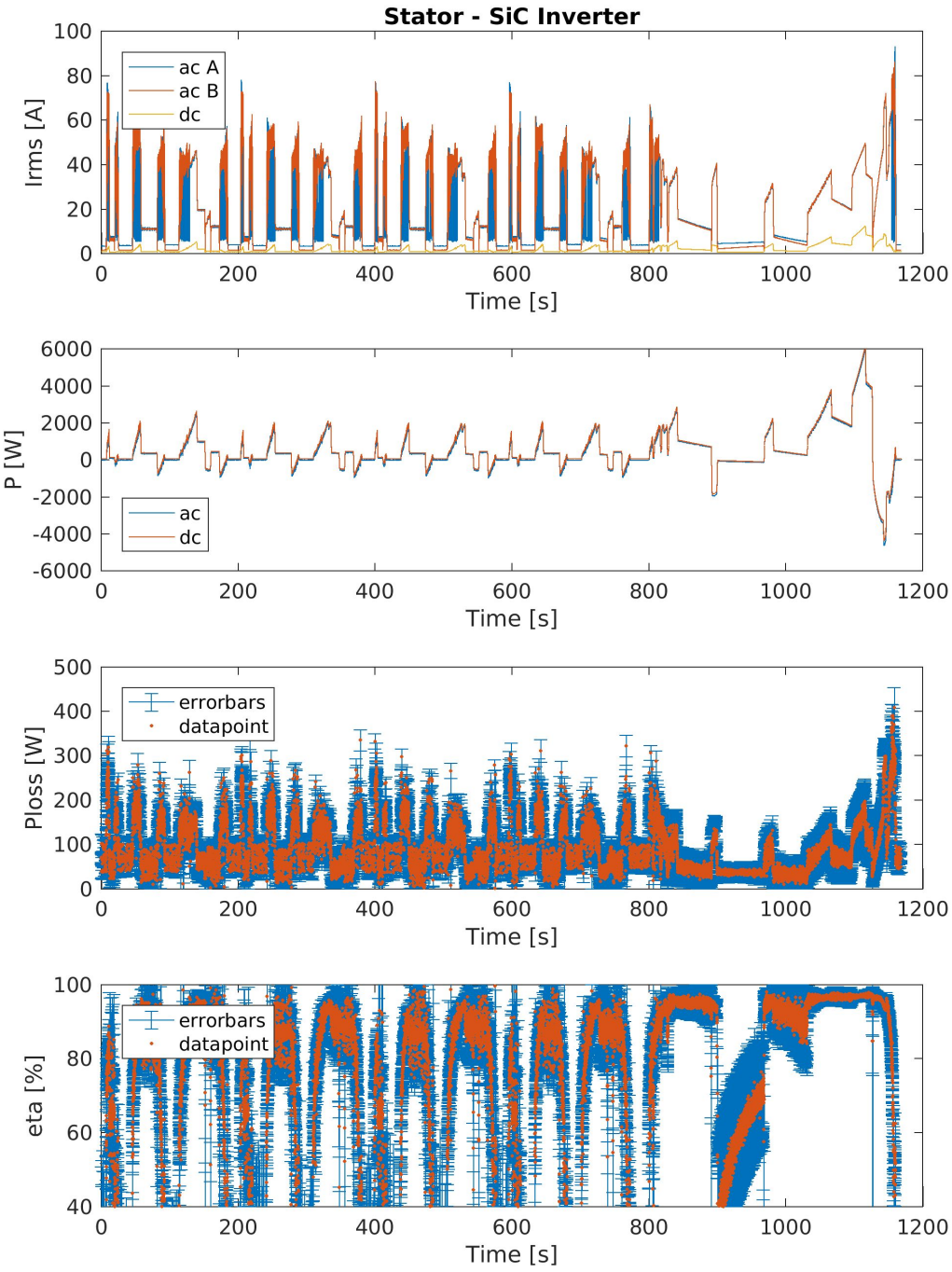

Fig. 8: Performance of the stator when the SiC MOSFET inverter is used.

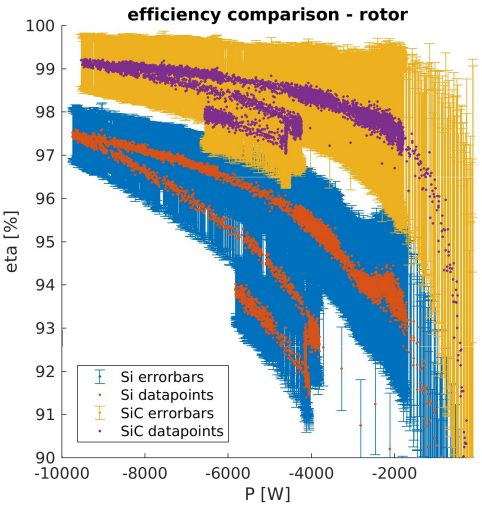

(a) Energy efficiency: 96.6% (SiC) and 92.9% (Si).

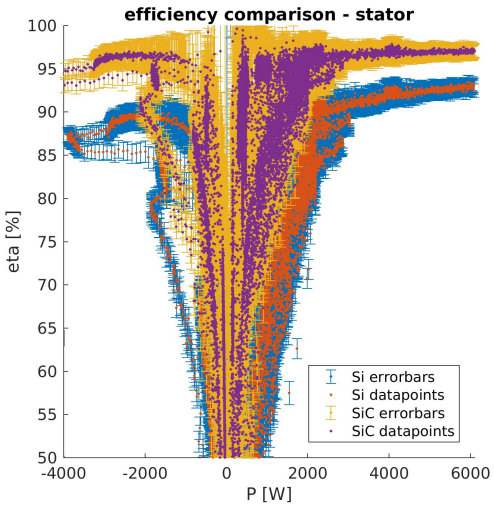

(b) Energy efficiency: 88.8% (SiC) and 77.6% (Si).

Fig. 9: Efficiency comparison of SiC vs Si inverters connected to the inner rotor/stator.

References

[1] M. Hoeijmakers and J. Ferreira, "The electric variable transmission", IEEE Transactions on Industrial Applications, 42 (4), 2006, pp. 1092-1100.

[2] F. Verbelen, A. Abdallh, H. Vansompel, K. Stockman and P. Sergeant, "Sizing Methodology based on Scaling Laws for a Permanent Magnet Electrical Variable Transmission", IEEE Transactions on Industrial Electronics, 67 (3), 2019, pp. 1739-1749.

[3] M. Hoeijmakers, "Electromechanical converter, Patent US 7 164 219", 2007.

[4] E. Vinot, R. Trigui, Y. Cheng, C. Espanet, A. Bouscayrol and V. Reinbold, "Improvement of an EVT-Based HEV Using Dynamic Programming", IEEE Transactions on Vehicular Technology, 63 (1), 2014, pp. 40-50.

[5] P. Shamsi, M. McDonough and B. Fahimi, "Wide-Bandgap Semiconductor Technology: Its impact on the electrification of the transportation industry.," in IEEE Electrification Magazine, vol. 1, no. 2, pp. 59-63, Dec. 2013, doi: 10.1109/MELE.2013.2293931.

[6] Dalla Vecchia, M.; Ravyts, S.; Van den Broeck, G.; Driesen, J. Gallium-Nitride Semiconductor Technology and Its Practical Design Challenges in Power Electronics Applications: An Overview. Energies 2019, 12, 2663.

[7] A. Anthon, Z. Zhang, M. A. E. Andersen, D. G. Holmes, B. McGrath and C. A. Teixeira, "The Benefits of SiC mosfets in a T-Type Inverter for Grid-Tie Applications," in IEEE Transactions on Power Electronics, vol. 32, no. 4, pp. 2808-2821, April 2017, doi: 10.1109/TPEL.2016.2582344.

[8] D. Sadik et al., "Short-Circuit Protection Circuits for Silicon-Carbide Power Transistors," in IEEE Transactions on Industrial Electronics, vol. 63, no. 4, pp. 1995-2004, April 2016, doi: 10.1109/TIE.2015.2506628.

[9] J. Druant, H. Vansompel, F. De Belie, J. Melkebeek and P. Sergeant, "Torque Analysis on a Double Rotor Electrical Variable Transmission With Hybrid Excitation", IEEE Transactions on Industrial Electronics, 64 (1), 2017, pp. 60-68.

[10] J. Druant, H. Vansompel, F. De Belie and P. Sergeant, "Optimal Control for a Hybrid Excited Dual Mechanical Port Electric Machine", IEEE Transactions on Energy Conversion, 32 (2), 2017, pp. 599-607.

[11] J. Druant, H. Vansompel, F. De Belie, and P. Sergeant, "Loss Identification in a Double Rotor Electrical Variable Transmission", IEEE Transactions on industrial electronics, 64 (10), 2017, pp. 7731–7740.

[12] M. Vafaeipour, M. El Baghdadi, J. Van Mierlo, O. Hegazy, F. Verbelen and P. Sergeant, "An ECMS-based approach for energy management of a HEV equipped with an electrical variable transmission", Fourteenth International Conference on Ecological Vehicles and Renewable Energies (EVER), 2019.

[13] JCGM 100:2008 "Evaluation of measurement data — Guide to the expression of uncertainty in measurement"